Efficient Seismic Risk Analysis: Disaggregation-based Weighting of Non-linear Dynamic Analysis Results

L. Elefante, F. Jalayer , I. Iervolino & G. Manfredi
Dipartimento di Ingegneria Strutturale, Università degli Studi di Napoli Federico II

ABSTRACT:
Ground motion (GM) record selection represents one of the main issues in assessing the seismic response of a structure through numerical dynamic analysis. In the framework of the probabilistic performance-based assessment it is useful to introduce an intermediate parameter (scalar or vector), known as the ground motion *intensity measure IM,* to relate the GM record characteristics to the structural performance. This approach often assumes that structural response depends only upon the chosen *IM*, which is believed to carry the largest information with respect to other properties of the GM. This condition is termed "sufficiency" and must be carefully verified since, if it is not met, then the probability distribution for the damage measure will not only depend upon *IM*, but also upon the (other) properties of the records selected for analysis. In principle, careful record selection is not essential if the *IM* is demonstrated to be sufficient with respect to GM characteristics. However, establishing the sufficiency of an *IM* is not a trivial task and may be structure and/or response measure dependent.
In cases where the *IM* is not sufficient, the GM record selection may be guided by the disaggregation of the seismic hazard for the site of interest. The results of seismic hazard disaggregation can be used to assign relative weights to a given GM record based on the likelihood that a GM having its corresponding magnitude, distance and deviation from the GM prediction model (*epsilon*) actually occurs. The weighted GMs can be used in order to make probability-based seismic assessments using non-linear dynamic analysis procedure both for a wide and a limited range of GM intensities.
In this paper, the implications of using the weighted GM records are investigated in terms of seismic risk, which is represented herein by the mean annual frequency of exceeding the critical structural component demand to capacity ratio, in an existing reinforced concrete structure using both the peak ground acceleration and the first-mode spectral acceleration as *IM*s. It is demonstrated that the annual frequencies based on weighted records are comparable to those obtained using vector-valued intensity measures, yet requiring less computational effort.

Keywords: intensity measure; non-linear dynamic analysis; weighted regression; seismic hazard disaggregation.

1. INTRODUCTION

In non-linear dynamic analysis procedures, the choice of seismic input may be affected by the interface variable used to measure the intensity of GM, known as the intensity measure *IM*. According to criteria proposed by Luco and Cornell (2003) a preferred *IM* is both "sufficient" with respect to the GM characteristics and also "efficient". A sufficient *IM* renders the structural response conditionally statistically independent of other GM characteristics, while an efficient *IM* predicts the structural response with (comparatively) small record-to-record variability. In principle, careful record selection is not essential if the *IM* is demonstrated to be sufficient (Iervolino and Cornell 2005). An useful strategy, in cases where the adopted scalar intensity measure IM_1 does not prove to be sufficient, is to introduce an additional intensity measure, IM_2 adopting a vector-valued $\boldsymbol{IM}=[IM_1,IM_2]$ in order to render a more complete description of the GM characteristics (Baker and Cornell 2005).
In this paper, an approximate method based on linear regression is used in order to establish possible correlation between the structural response conditional on the primary IM_1 and the secondary IM_2.

Moreover, a weighting scheme based on seismic hazard disaggregation (Bazzurro and Cornell, 1999) is used, in the framework of the scalar IM_1, for both wide and limited range of GM intensities, in order to adjust the structural response for possible correlations with a candidate secondary IM_2.The efficiency of the weighting scheme is evaluated in terms of seismic risk which is represented herein by the mean annual frequency of exceeding the critical component demand to capacity ratio.

2. PROBABILISTIC ASSESSMENT BASED ON NON-LINEAR DYNAMIC ANALYSIS

Adopting the performance assessment methodology developed by the Pacific Earthquake Engineering Research (PEER) Center for buildings, a probabilistic performance-based criterion for seismic assessment of existing structures is:

$$\lambda_{EDP} \leq P_0 \tag{2.1}$$

where λ_{EDP} is the (mean) annual frequency (MAF) of exceeding a specified damage level expressed in terms of an engineering demand parameter (*EDP*) and P_0 is the allowable probability threshold for the assessment[1]. In this framework, an intermediate parameter known as the intensity measure *IM* is introduced in order to relate the characteristics of the GM record to structural performance. The MAF of exceeding a specified limit state can be expanded, using probability theory, with respect to *IM* in the following (Vamvatsikos and Cornell 2001; Jalayer and Cornell, 2009):

$$\lambda_{EDP}(y) = \int P_{EDP|IM_1}\left(EDP > y|x, z\right)\left|d\lambda_{IM_1}(x)\right| \tag{2.2}$$

The first term in the integrand $P_{EDP|IM}(EDP > y|x)$ is the conditional probability of exceeding the structural response threshold y for $IM=x$. This term is also known as the structural *fragility*. The second term in the integrand is the absolute value of the derivative of the annual rate of exceeding $IM=x$; this second term is known as the *hazard* for the adopted *IM*.

The non-linear dynamic analysis procedures based on a limited suite of GM records can be used to estimate the fragility term in equation 2.2. Depending on the amount of structural analysis, two alternative non-linear dynamic analysis procedures are considered in this work, the *cloud method* and the *stripes method*. Both procedures assume a Gaussian distribution for the logarithm of *EDP* given *IM*.

The cloud method employs the linear least squares scheme to the specified *EDP* given *IM* based on non-linear structural response (*cloud response*) for a suite of GM records (un-scaled) in order to estimate the conditional mean and standard deviation of *EDP* given *IM*.

The stripes method provides the non-linear structural response parameters for the suite of records that are scaled to successively increasing *IM* levels: this is referred to as the *stripe response*; the statistical properties of the stripe response are calculated for various *IM*.

In the case where a vector-valued $\boldsymbol{IM}=[IM_1,IM_2]$ consisting of two scalar *IM*'s is adopted, the fragility term can be expanded with respect to IM_2 and re-arranged as following (Baker, 2007):

$$\lambda_{EDP}(y) = \iint P_{EDP|IM_2,IM_1}\left(EDP > y|x, z\right) f_{IM_2|IM_1}\left(z|x\right)\left|d\lambda_{IM_1}(x)\right| \tag{2.3}$$

The first term in the integrand is the conditional probability of exceeding $EDP=y$ given IM_1 and IM_2 and the second term is the conditional probability density function (PDF) for $IM_2=z$ given $IM_1=x$.

In this work, both scalar and vector *IM*'s are studied. As scalar *IM*'s, the peak ground acceleration (PGA) and the first-mode spectral acceleration ($S_a(T_1)$) are considered. As vector *IM*'s, the pairs consisting of PGA and magnitude M (Jalayer, 2003), $S_a(T_1)$ and the deviation from the GM prediction model epsilon (ε) (Baker and Cornell 2005) are considered. Epsilon is defined as the number of standard deviations by which an observed logarithmic spectral acceleration differs from the mean logarithmic spectral acceleration of a ground-motion prediction (attenuation) equation.

[1] Note that in equation 2.1 it has been assumed that the numerical value of annual rate of exceedance is close to that of the probability of exceedance, which is acceptable if the latter is small.

The *EDP* can be defined as a functional of component demand and capacities, which is equal to one at the onset of failure.
The formulation adopted herein is based on the system reliability concept of *cut-sets* (Ditelvsen and Masden 1996). The scalar global *EDP*, denoted by Y (Jalayer et al., 2007), is a critical demand to capacity ratio defined as the demand to capacity ratio of the strongest component of the weakest structural mechanism or cut-set:

$$Y = \max_{l=1}^{N_{mech}} \min_{j=1}^{N_l} \frac{D_{jl}}{C_{jl}} \tag{2.4}$$

where N_{mech} is the number of considered cut-sets or potential failure mechanisms and N_l is the number of components taking part in the l^{th} cut-set. A cut-set is defined as any set of components whose joint failure leads to system failure.

3. STRUCTURAL MODEL

As the case-study, an existing school structure in the city of Avellino, Italy, is considered herein. The structure consists of three stories and a semi-embedded story, and its foundation lies on stiff soil (category B according to Eurocode 8, CEN 2003). The building was constructed in the 1960's and it is designed for gravity loads only, as it is frequently encountered in the post second world war construction. The main central frame in the structure is extracted and used as the structural model (Figure 1a).

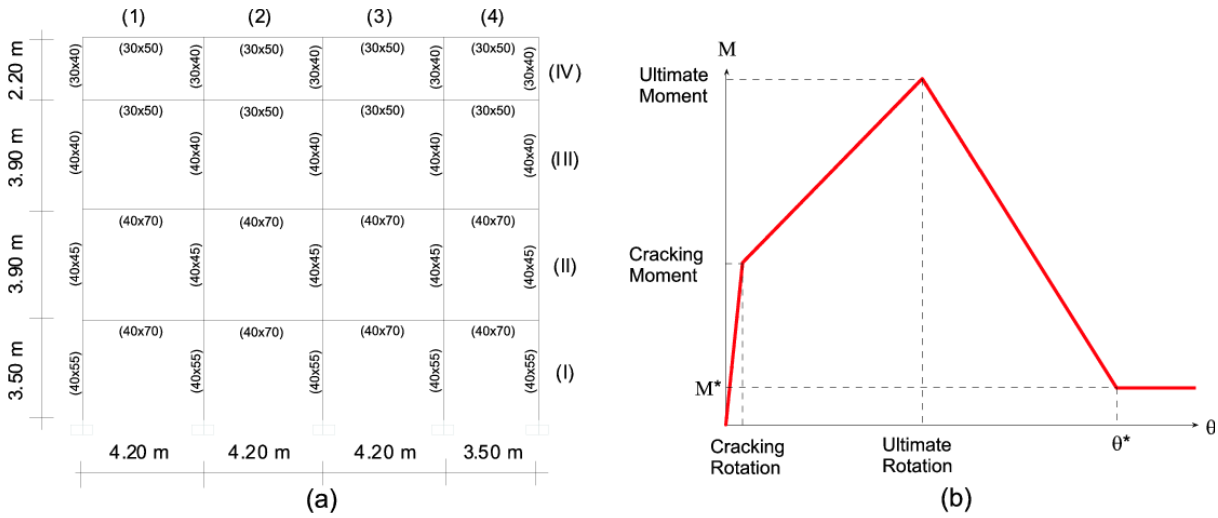

Figure 1. (a) The central frame of the case-study building. (b) Schematic diagram of the typical tri-linear behavior characterizing the plastic hinge.

The steel yield resistance and the concrete compression resistance in the structural model are taken equal to 3200 kg/cm^2 and 165 kg/cm^2, respectively: these are mean values extracted from a statistical survey of material properties in existing buildings constructed in the 1960's (Verderame et al., 2001a - b).
The finite element model of the frame is constructed, using the Open System for Earthquake Engineering Simulation (OpenSees) software, assuming that the non-linear behavior in the structure is concentrated in plastic hinges located at the element ends (Scott and Fenves 2006). The concrete behavior is modeled based on the Mander-Priestly (Mander et al., 1988) constitutive relation for un-confined concrete. The reinforcing steel is assumed to have elastic-plastic behavior. The tri-linear moment-rotation backbone curve is demonstrated in Figure 1b[2]. The structural damping is modeled

[2] These post-peak values for moment and rotation are chosen rather arbitrarily in order to avoid numerical in-convergence problems ($M^*=0.1 \cdot M_u$; $\theta^*=2 \cdot \theta_u$).

based on the Rayleigh model and is assumed to be equal to 5% for the first two modes. The small-amplitude period for the first two vibration modes are equal to 0.73 and 0.26 seconds respectively.

4. THE SUITES OF GROUND MOTION RECORDS AND THEIR PROPERTIES

Two different suites, respectively of 21 (*Sel_A*) and 20 (*Sel_B*) GM records, all based on Mediterranean events, have been selected for this study. They are all main-shock recordings recorded on stiff soil (400 m/s < V_{s30} < 700 m/s) which is consistent with the soil-type of the site. The two suites of records are taken from European Strong-motion (ESD) (http://www.isesd.cv.ic.ac.uk/ESD/Database/Database.htm) and PEER Next Generation Attenuation (NGA) (http://peer.berkeley.edu/nga/flatfile.html) Database in order to cover a wide range of moment magnitude M_w values (*Sel_A*) and ε values (*Sel_B*).
Table 4.1 illustrates the GM recordings, their M_w, epicentral distance (ED), PGA, $S_a(T_1)$) and ε values for each record of *Sel_A* (left side) and *Sel_B* (right side) respectively.

Table 4.1. Selection A and selection B of ground motion records.

Sel_A	M_w	ED [km]	PGA [g]	$S_a(T_1)$ [g]	ε	*Sel_B*	M_w	ED [km]	PGA [g]	$S_a(T_1)$ [g]	ε
Basso Tirreno	6.0	18	0.15	0.17	-0.121	Friuli	6.5	42	0.06	0.22	-0.015
Valnerina	5.8	23	0.04	0.03	-0.529	Friuli	6.5	87	0.05	0.11	0.003
Cam. Lucano	6.9	16	0.16	0.31	-0.519	Cam. Lucano	6.9	48	0.11	0.25	-0.204
Preveza	5.4	28	0.14	0.10	-0.244	Cam. Lucano	6.9	16	0.16	0.31	-0.493
Umbria	5.6	19	0.21	0.02	0.230	Kalamata	5.9	10	0.22	0.48	-0.231
Laz. Abruzzo	5.9	36	0.07	0.05	-0.219	Kalamata	5.9	11	0.24	0.48	-0.233
Etolia	5.3	20	0.04	0.01	-0.518	Umb. Marche	6.0	11	0.52	0.56	-0.216
Montenegro	5.4	18	0.07	0.09	-0.227	Umb. Marche	6.0	38	0.09	0.17	0.062
Kyllini	5.9	14	0.15	0.15	-0.231	South Iceland	6.5	7	0.63	0.54	-0.288
Duzce 1	7.2	26	0.13	0.18	-0.722	Duzce 1	7.2	26	0.13	0.18	-0.893
Umb. Marche	5.7	32	0.04	0.05	-0.334	Friuli	6.5	42	0.09	0.25	0.031
Potenza	5.8	28	0.10	0.08	-0.003	Friuli	6.5	87	0.07	0.12	-0.002
Ano Liosia	6.0	20	0.16	0.06	-0.308	Cam. Lucano	6.9	48	0.14	0.26	-0.187
Adana	6.3	39	0.03	0.05	-0.749	Cam. Lucano	6.9	16	0.18	0.31	-0.484
South Iceland	6.5	15	0.21	0.13	-0.344	Kalamata	5.9	10	0.30	0.63	-0.120
Tithorea	5.9	25	0.03	0.02	-0.639	Kalamata	5.9	11	0.27	0.51	-0.208
Patras	5.6	30	0.05	0.02	-0.184	Umb. Marche	6.0	11	0.46	0.64	-0.156
Friuli Italy1	6.5	20	0.35	0.35	0.168	Umb. Marche	6.0	38	0.10	0.18	0.065
Friuli Italy2	5.9	18	0.21	0.08	0.110	South Iceland	6.5	7	0.51	0.74	-0.154
Friuli Italy3	5.5	20	0.11	0.21	0.034	Duzce 1	7.2	26	0.16	0.14	-1.004
Irpinia Italy1	6.9	15	0.13	0.30	-0.466	*average*	6.4	30	0.22	0.35	-0.236
average	6.0	23	0.12	0.12	-0.277						

In order to adopt a vector-valued ***IM*** for representing the GM intensity in the seismic assessment outlined in equation 2.3, it is necessary to obtain the conditional probability distribution for the second *IM* (IM_2) given the occurrence of the original *IM* (IM_1).
A site-specific seismic hazard analysis is performed based on the Italian seismic zonation (ZS9, Meletti et al., 2008) inside a Bayesian framework for inference in order to obtain the conditional probability distribution for magnitude m, distance r and the deviation from the attenuation law ε given IM_1. The GM prediction relation adopted in this work is the Sabetta and Pugliese relation (Sabetta and Pugliese, 1996). Through the disaggregation of the seismic hazard for the site of the case-study structure, the conditional probability distributions of M given PGA and ε given $S_a(T_1)$, have been obtained.

5. RESIDUAL-RESIDUAL PLOT AND THE WEIGHTED METHOD

In this study, a simplified statistical approach based on regression is implemented for measuring the effectiveness of GM characteristics as additional regression variables. This method uses a graphical statistical tool known as the residual-residual plot. Residual-residual plots are constructed by: a) performing regression of the dependent variable EDP versus the (first) independent variable IM_1 (e.g., PGA or $S_a(T_1)$), b) performing regression of the second independent variable IM_2 (e.g., M or ε) on the first variable IM_1, c) plotting the residuals of the two regressions mentioned above against each other. The main advantage of the residual-residual plots is that they offer visual means for judging the improvement caused by an additional regression variable by observing a (statistically) significant trend, in the linear regression between the two sets of residuals. Through hypotheses test it is possible to evaluate if the *IM* introduced reduces the variability of results than the original prediction of regression. A weighted regression scheme is used herein as it may help in reducing the dependence of the residuals on IM_2; its weights each error term (residual) proportional to its corresponding variance (Rice, 1995). It can be argued that the variance of each error term and hence the corresponding weight is positively related to the following ratio:

$$w_i \propto \frac{f_{IM_2|IM_1}\left(z_i|x\right)_{disaggregation}}{f_{IM_2|IM_1}\left(z_i|x\right)_{data}} \tag{5.1}$$

where $f_{IM_2|IM_1}\left(z|x\right)$ is the fraction of the GMs with IM_2 equal to z for a given IM_1 equal to x. In this work, it is assumed that it is equally likely to observe IM_2 given IM_1 for each record in the set; therefore, $f_{IM_2|IM_1}\left(z_i|x\right)_{data}$ is going to be equal to $1/N_T$, where N_T is the total number of records. $f_{IM_2|IM_1}\left(z_i|x\right)_{disaggregation}$ is the probability that IM_2 is equal to z_i for a given IM_1 equal to x, estimated by disaggregation of seismic hazard. A similar procedure can be implemented in the framework of the multiple-stripe analysis, after having discretizing IM_2 into a set of bins. In fact, for a given suite of GM records, the stripe response at each IM_1 level can be weighted in relation to the conditional probability distribution $f(IM_2|IM_1)$ (Shome and Cornell, 1999).

In this study, the logistic regression (Neter et al., 1996) is applied to the collapse data in order to predict the probability of collapse as a function of the second IM_2. Using the indicator variable C to designate occurrence of collapse (C equals 1 if the record causes collapse and 0 otherwise), the following functional form is fitted (Baker, 2007):

$$P\left(C|IM_1 = x, IM_2 = z\right) = \frac{e^{a(x)+b(x)\cdot z}}{1+e^{a(x)+b(x)\cdot z}} \tag{5.2}$$

where a and b are coefficients to be estimated for the stripe response at $IM_1=x$. Using the total probability theorem the first term in the integrand of equation 2.3 can be expanded in this way:

$$P_{EDP|IM_1,IM_2}(EDP > y|x,z) = P_{EDP|IM_1,IM_2}(EDP > y|x,z,NC)P(NC|x,z) + 1 \cdot P(C|x,z) \tag{5.3}$$

where $P(NC|x,z) = 1 - P(C|x,z)$ is the probability of not having collapses (NC) given $IM_1=x$ and $IM_2=z$.

6. NUMERICAL RESULTS

6.1. The Cloud Method

In Figure 3a and 3c the residual-residual plot related to the introduction of M (for *Sel_A*) and ε (for *Sel_B*) as IM_2, together with the *p*-values calculated for the hypotheses test are shown. A significant trend in the plots can be observed: this means that PGA (for *Sel_A*) and $S_a(T_1)$ (for *Sel_B*) are not sufficient with respect to M and ε respectively. In Figure 3b and 3d the results obtained using the weighted regression scheme, based on the results of seismic hazard disaggregation, are shown; the results of structural analysis are plotted by circles with areas proportional to the corresponding weight. The dashed lines are obtained with the weighted regression scheme, instead, the thin lines are obtained with the simple regression scheme.

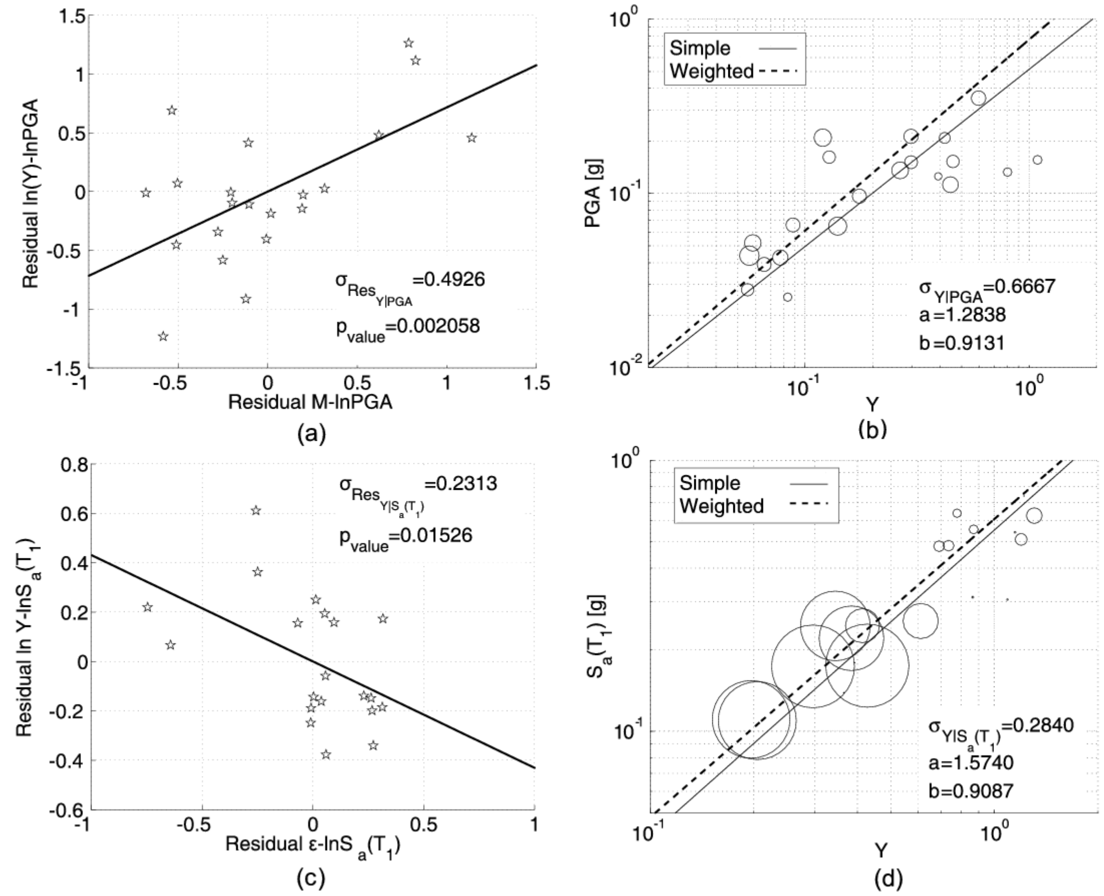

Figure 3. (a) Residual-residual plot for the introduction of M as IM_2, *Sel_A* (b) Simple regression Y-PGA and weighted regression PGA-M-Y, *Sel_A*. (a) Residual-residual plot for the introduction of ε as IM_2, *Sel_B* (b) Simple regression Y- $S_a(T_1)$ and weighted regression $S_a(T_1)$- ε-Y, *Sel_B*.

It would be interesting to study how the seismic risk, represented herein by the MAF of exceeding Y, is affected by the weighed regression scheme (Figure 4).

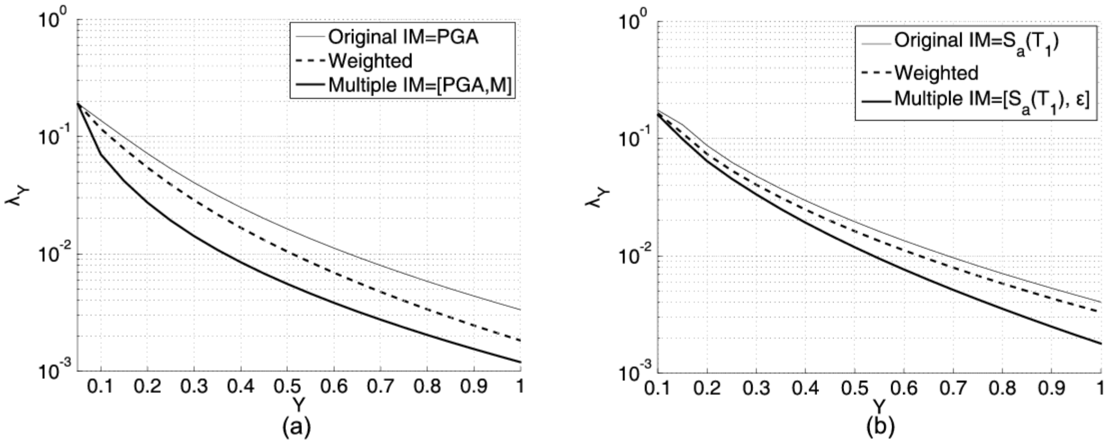

Figure 4. (a) The MAF of exceeding Y, *Sel_A*. (b) The MAF of exceeding Y, *Sel_B*.

In Figures 4a and 4b the thick lines represent the MAF of exceeding the Y adopting as ***IM*** the pair [PGA, M] and [$S_a(T_1)$, ε], for *Sel_A* and for *Sel_B*, respectively. The thin lines represent the MAF of exceeding Y using a scalar IM_1 (PGA for *Sel_A* and $S_a(T_1)$ for *Sel_B*). The dashed lines represent the MAF of exceeding Y using a scalar IM_1 (PGA for *Sel_A* and $S_a(T_1)$ for *Sel_B*) but adjusting for the dependence on IM_2 (M for *Sel_A*, ε for *Sel_B*) by weighted regression. It can be observed that the weighted regression manages to take into account some of the information provided by IM_2 and its corresponding MAF of exceeding Y ends up somewhere between those corresponding to the original cloud method and the multiple-regression, respectively

6.2. The Multiple-Stripe Analysis

Figures 5a and 5b illustrate the results of multiple-stripe analysis, using the same *IM*'s adopted in the cloud method, for the case-study structure subjected to *Sel_A* and *Sel_B* respectively. The number of "collapse cases" encountered for each *IM* level and the lines connecting the (counted) 16th, 50th and 84th percentiles of the stripe response at each *IM* level are also shown.

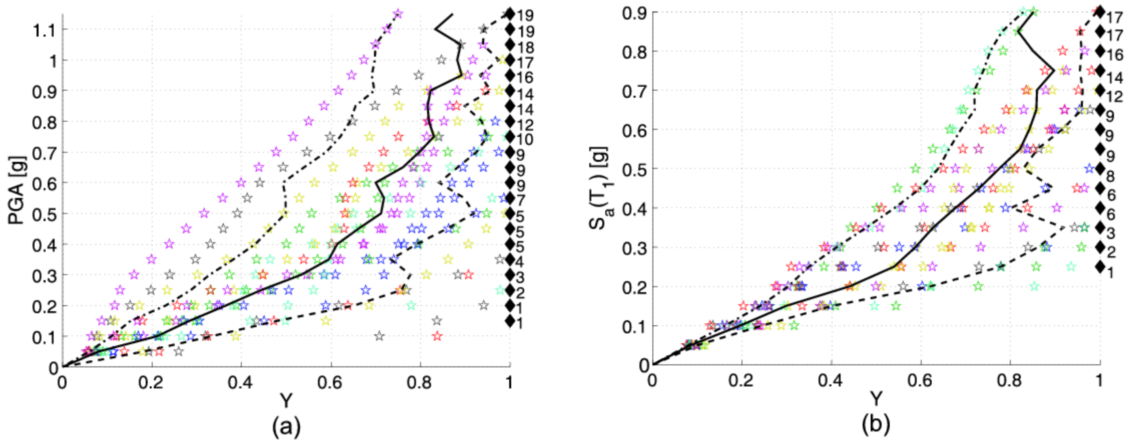

Figure 5. (a) Results of multiple stripe analysis for *Sel_A*. (b) Results of multiple stripe analysis for *Sel_B*.

Through numerical integration of the structural fragility with the *IM* hazard curve, the seismic risk curves for the critical component demand to capacity are calculated (Figure 6a and 6b). Similar to cloud method, the results of the multiple-stripe method indicate that seismic risk curve obtained using the weighted scheme is reasonably close to that based on multiple regression.

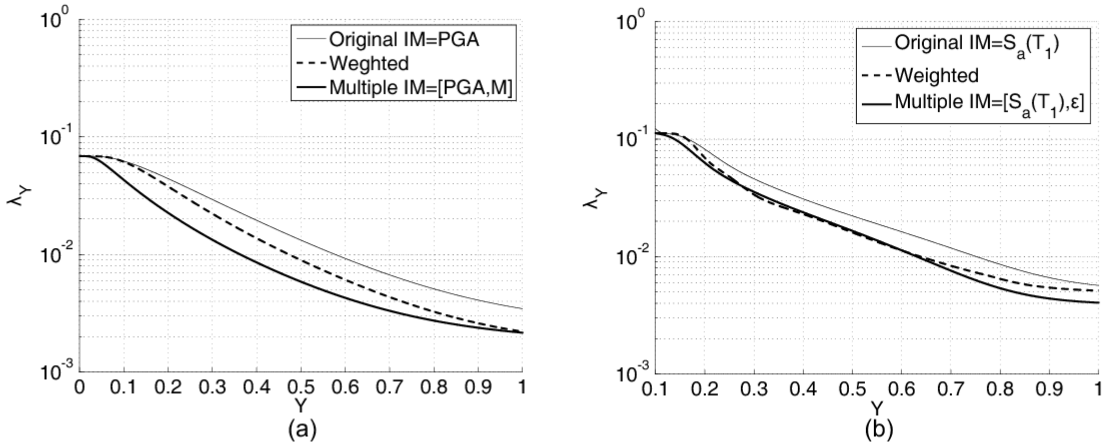

Figure 6. (a) The MAF of exceeding Y, *Sel_A*. (b) The MAF of exceeding Y, *Sel_B*.

7. CONCLUSIONS

A simple statistical/graphical tool known as the residual-residual plot is employed in this work in order to reveal possible dependence of the *EDP* conditional on the adopted IM_1, on a candidate IM_2. In cases where sufficiency for IM_1 is not established, a weighting scheme based on the results of the seismic hazard analysis can be adopted in order to implement the additional information provided by a candidate IM_2. The conditional probability distributions $f(\mathrm{M}|\mathrm{PGA})$ and $f(\varepsilon|S_a(T_1))$ have been calculated through the disaggregation of the seismic hazard for the site of the case-study structure using the Bayesian updating. Two alternative non-linear dynamic analysis procedures, the cloud method and the multiple-stripe method have been considered in this work.

The implication of using the weighting scheme has been studied in terms of seismic risk represented herein by the MAF of exceeding the critical component demand to capacity ratio Y. The seismic risk curves obtained by adopting the scalar IM_1 and the vector-valued $\boldsymbol{IM}=[IM_1,IM_2]$ are used to benchmark the efficiency of the weighting scheme. It is observed that the weighting scheme manages to take into account some of the information provided by IM_2 and its corresponding MAF of exceeding Y ends up somewhere between those obtained adopting the scalar IM_1 and the vector-valued $\boldsymbol{IM}=[IM_1,IM_2]$. In this case-study, the weighting scheme proves to be more efficient for multiple-stripe analysis compared to the cloud analysis. This can be attributed to the fact that, the multiple-stripe analysis spans over a wider range of *IM* levels and therefore may be less sensitive to the selection of GM records.

REFERENCES

Luco N. and Cornell C.A. (2003). Structure-Specific Scalar Intensity Measures for Near-Source and Ordinary Earthquake Ground Motions, *Earthquake Spectra*, **23(2)**: pp. 357-392.

Iervolino I. and Cornell C.A. (2005). Record selection for nonlinear seismic analysis of structures. *Earthquake Spectra*, **21(3)**: pp. 685-713.

Baker J.W. and Cornell C.A. (2005). A vector-valued ground motion intensity measure consisting of spectral acceleration and epsilon. *Earthquake Engineering & Structural Dynamics*, **34**: pp. 1193-1217.

Bazzurro P. and Cornell C.A. (1999). Disaggregation of seismic hazard, *Bulletin of the Seismological Society of America*, **89(2)**: pp. 501-520.

Vamvatsikos D. and Cornell C.A. (2001). Incremental dynamic analysis, *Earthquake Engineering and Structural Dynamics*, **31(3)**: pp. 491-514.

Jalayer F. and Cornell C.A. (2009). Alternative Nonlinear Demand Estimation Methods for Probability- Based Seismic Assessments, *Earthquake Engineering and Structural Dynamics*, **38(8)**: pp. 951-972.

Baker J.W. (2007). Probabilistic structural response assessment using vector-valued intensity measures. *Earthquake Engineering & Structural Dynamics*, **36(13)**: pp. 1861-1883.

Jalayer F. (2003). *Direct Probabilistic Seismic Analysis: Implementing Non-linear Dynamic Assessments*, Ph.D. Thesis, Department of Civil and Environmental Engineering, Stanford, CA.

Ditlevsen O, Masden H. (1996). *Structural Reliability Methods*, John Wiley & Sons Inc.

Jalayer F., Franchin P. and Pinto P.E. (2007). A Scalar Decision Variable for Seismic Reliability Analysis of RC Frames, *Special issue of Earthquake Engineering and Structural Dynamics on Structural Reliability*, **36(13)**: pp. 2050-2079.

CEN, European Committee for Standardisation TC250/SC8/ [2003] “Eurocode 8: Design Provisions for Earthquake Resistance of Structures, Part 1.1: General rules, seismic actions and rules for buildings”, PrEN1998-1.

Verderame G.M., Stella A., Cosenza E. (2001). “Le proprietà meccaniche degli acciai impiegati nelle strutture in cemento armato realizzate negli anni ’60”, *X Convegno Nazionale "L'Ingegneria Sismica in Italia"*, Potenza e Matera 9-13 Settembre 2001b (*in italian*).

Verderame G.M., Manfredi G., Frunzio G. (2001) “Le proprietà meccaniche dei calcestruzzi impiegati nelle strutture in cemento armato realizzate negli anni ’60”, *X Congresso Nazionale “L’ingegneria Sismica in Italia”*, Potenza-Matera 9-13 settembre 2001a (*in italian*).

Scott M.H. and Fenves G.L. (2006). Plastic hinge integration methods for force-based beam-column elements, *Journal of Structural Engineering, ASCE*, **132(2)**: pp. 244-252.

Mander J.B., Priestley M.J.N., Park R. (1988). Theoretical stress-strain model for confined concrete, *Journal of Structural Engineering*, **114(8)**: pp. 1804-1826.

Meletti C., Galadini F., Valensise G., Stucchi M., Basili R., Barba S., Vannucci G., and Boschi E. (2008). A seismic source zone model for the seismic hazard assessment of the Italian territory, *Tectonophysics,* **450**: pp. 85–108.

Sabetta F. and Pugliese A. (1996). Estimation of response spectra and simulation of non-stationary earthquake ground motions. *Bulletin of the Seismological Society of America*, **86(2)**: pp. 337-352.

Rice J. A. (1995) *Mathematical Statistics and Data Analysis*, Belmont, CA: Duxbury/Wadsworth.

Shome N. and Cornell C.A. (1999). *Probabilistic seismic demand analysis of non-linear structures.* Report No. RMS-35, Stanford University, Stanford, CA.

Neter J., Kutner M. H., Nachtsheim C. J. and Wasserman W. (1996). *Applied linear statistical models*, McGraw-Hill, Boston.